A 10 nW, 10 mV Signal Detector Using a 2 pA Standby Voltage Reference, for Always-on Sensors and Receivers

Salah-Eddine Adami, Guang Yang, Chunhong Zhang, Plamen Proynov, Bernard H. Stark
Faculty of Engineering, University of Bristol, Bristol, UK
bernard.stark@bristol.ac.uk

Abstract— **An RF energy harvesting circuit is usually designed to maximise efficiency and therefore output power, while a passive wake-up radio is usually optimised for a high open-circuit output voltage resulting in high sensitivity. These two functions have conflicting design requirements, but are generally both needed in Internet-of-Things devices. This paper presents a new approach to holding almost the entire system fully powered down whilst listening, whilst also obtaining an effective wake-up and energy harvesting circuit using the same rectenna (rectifying antenna). The topology uses a rectenna that is optimised for efficiency, and two signal detector circuits that draw up to 3.5 nA from the battery. One detector is configured to trigger at 85 mV, to start up the boost converter when enough power is available to obtain net-positive energy harvesting. The other detector is set to be more sensitive, to wake up subsystems when the rectenna output reaches 10 mV. The detector architecture and transistor-level design are presented, and the detection threshold and power levels experimentally verified. The circuit draws 10 nW at a sensitivity of 10 mV, and 3.9 nW at 85 mV. This detection system is the first reported circuit with a configurable detection threshold that draws only nW from the battery, and that, in addition to RF signals, can be used with any transient signals, such as outputs from piezoelectric sensors, microphones, or energy harvesters that produce in excess of around 10 mV. The low power consumption of this circuit is largely due to use of the UB20M voltage detector, whose internal on-demand voltage reference generator is also reported here. It has the lowest reported standby current of 2 pA, and a sub-microsecond-scale turn-on response time.**

Keywords—RF energy harvesting; RF wake-up; rectenna; boost converter; internet-of-things; sensors.

I. INTRODUCTION

RF energy harvesting is a promising way of powering the next generation of Internet-of-Things (IoT) sensor nodes. An important design goal in any energy harvesting application is the end-to-end efficiency from the source to the load. For RF energy harvesting, this includes the efficiencies of the rectifier and the dc-dc converter. Recent publications have shown considerable improvement in rectification efficiency down to very low RF power levels below -30 dBm [1]. Power electronic converters dedicated to energy harvesting have also seen a dramatic reduction in their minimum operating power, e.g. a dc power as low as 1.1 nW can be converted with a 53% efficiency [2].

This work was performed under the SPHERE IRC funded by the UK Engineering and Physical Sciences Research Council (EPSRC), Grant EP/K031910/1, and funds from EPSRC's Impact Acceleration Account.

Wake-up radio is another important function for low-power IoT sensors. These are typically very low-power always-on receivers that extract the baseband information from the RF signal, and process this data sequence in order to determine if system wake-up has been requested. A zero-power wake-up concept is reported in [3] that uses tens of passive voltage multiplier stages in CMOS technology. Increasing the number of stages in a voltage doubler usually improves the output open-circuit voltage, at the expense of power conversion efficiency. For that reason, especially if the RF power range is wide, a rectifier optimised for wake-up would not usually perform well as an energy harvester. Similar trade-offs are encountered with other types of energy harvesting sources.

This paper presents a design approach that permits the rectenna to be optimised for energy harvesting, i.e. efficiency, whist still having acceptable wake-on-radio sensitivity, for example for the remote control or testing of sensors. It also permits all but two detector circuits to be fully powered down whist the circuit is listening for RF signals. An always-on detection circuit is presented that uses anywhere between zero and 3.5 nA from the battery, to adjust the detection threshold between 0.6 V and 10 mV. These current levels are significantly below the internal self-discharge of small watch batteries, and therefore usually negligible. This low power consumption is enabled by a dynamic voltage threshold generator with a standby current of only 2 pA, contained in the UB20M voltage detector [4] by Sensor Driven. This detector has a base threshold of 0.6 V when unassisted by a battery, and a maximum input voltage of 20 V, due to its implementation in 180 nm HVCMOS by AMS.

Section II presents the system architecture, the detector architecture, and the transistor-level design and operating principles of the UB20M's internal voltage detector and voltage reference generator. Section III presents an experimental validation of the detection thresholds and power consumptions, and threshold stability information. Section IV compares the system with the literature, and draws conclusions.

II. Combined Wake-on-Radio and Energy Harvesting Circuit

A. System Architecture

The system diagram of the combined RF energy harvester and wake-on-radio circuit is shown in Fig. 1. A receiving antenna and 2.45 GHz rectifier provide power and information content to two subsystems. The first is an energy harvesting system that contains a boost converter and a 85 mV detector circuit. As the boost converter requires power to operate, it is fully power-gated off when insufficient power is available to charge the battery. The detector is configured to trigger the operation of the boost converter exactly when the RF input power becomes sufficient to guarantee net positive power flow into the battery. This corresponds to an input dc voltage of 85 mV (RF level of -23 dBm). The second system is a wake-on-radio receiver. All circuitry is fully powered down during listening, except for an always-on detector that has detection threshold of 10 mV (-34 dBm). This system can be used to activate various sub-systems of the receiver, such as a decoder. This 10 mV always-on detector draws 3.3 nA from the 3 V battery, whilst the 85 mV detector draws 1.3 nA.

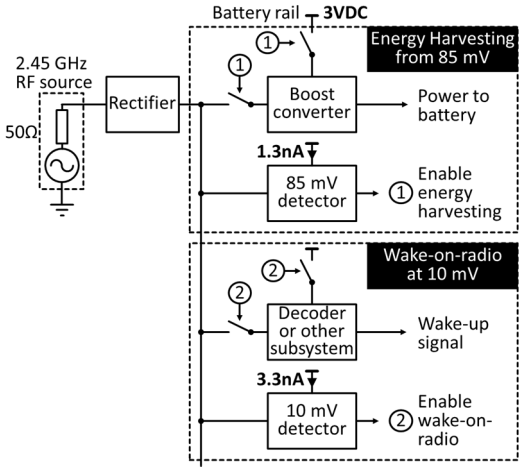

Fig. 1: Combined RF energy harvesting and wake-up circuit using always-on signal detectors to allow the rest of the system to be fully powered off.

B. Detector Architecture

Both detectors of Fig. 1 are implemented using the same architecture as shown in Fig. 2, with the only difference being their bias currents.

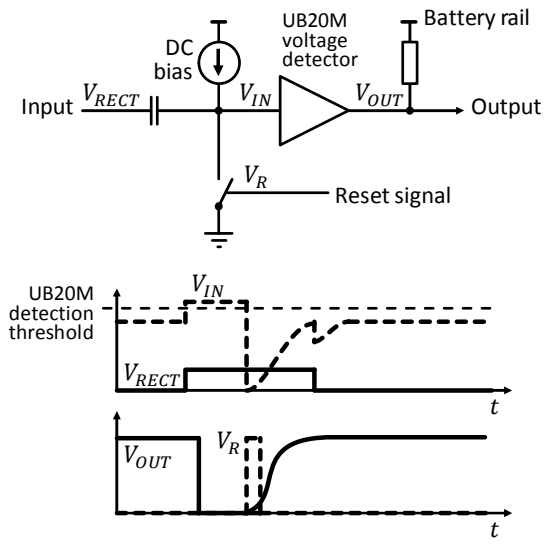

Fig. 2: Detector architecture and illustrative waveforms.

The circuit is based around an input-powered UB20M voltage detector IC [4] which does not require a supply rail. It has a detection threshold of 580 mV, an on-state current of 6 pA at room temperature, and a transient trigger current of around 3.1 nA at room temperature. In its off-state, the UB20M's output V_{OUT} is open circuit, and its output pulled up to the battery rail by a resistor, as seen in the illustrative waveforms of Fig. 2. The current through this resistor is determined by the voltage detector, and is below 100 pA. On a low-to-high transition at the input from the rectenna V_{RECT}, AC-coupled input V_{IN} transitions from its bias point through the UB20M's detection threshold, and the voltage detector enters its on-state where it consumes 10 pA from its input (40% of which is leakage into surrounding circuitry on the PCB). The output switches from open circuit to pulled down (inverting open-drain output). This high-to-low transition can be used to power-gate subsystems of a sensor node, using high-side p-channel FETs (not shown). Once the load has carried out its tasks, it feeds back a reset signal V_R to an n-channel FET to pull the input low and thus reset the voltage detector back into its off-state.

Fig. 3 shows the UB20M's input current against input voltage V_{IN}, and the operating points (listening, on, off) of the 10 mV detector. The supply of a bias current of just over 3 nA moves the listening point closer to the trigger point (3.1 nA, 580 mV), thus reducing the input signal amplitude of V_{RECT} needed to trigger the circuit.

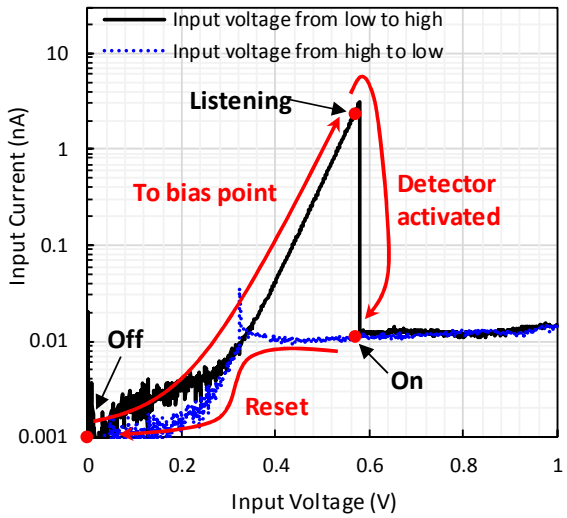

Fig. 3: Measured steady-state input current versus input voltage V_{IN} of the UB20M detector at room temperature. The peak of the I-V characteristic lies at the detection threshold voltage of 580 mV. The red dots represent the operating points of the 10 mV detector.

The 85 mV detector of Fig. 1 uses a bias current of 1.3 nA. Its operating point is therefore further from the detection threshold. Without bias current, the detector has a detection threshold of around 580 mV.

It is important that the bias current does not exceed the trigger current, or periodic wake-up is obtained.

C. *Input-Powered UB20M Voltage-Detector with Reset Function*

The functional blocks of the internal detector of the UB20M are shown in Fig. 4. There are three core functions: A subthreshold voltage reference, a trigger circuit, and output buffers. The output is fed back into the voltage reference to select the output voltage of the reference.

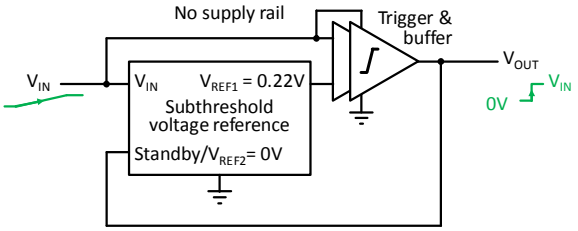

Fig. 4: Architecture of the internal detector in the UB20M. The subthreshold voltage reference has two possible output voltages, V_{REF1}= 0.22V and V_{REF2} = 0 V. Feedback from the output resets the voltage reference: as V_{OUT} goes high, the reference enters standby and outputs V_{REF2}.

The subthreshold voltage reference generates a fixed output V_{REF} of 0.22 V. The trigger is the decision-making circuit. It consists of an inverter, whose input is the constant reference V_{REF}, while its supply is the varying detector input voltage V_{IN}. The trigger switches its output to high as the supply rail V_{IN} reaches the detection threshold V_{TH}. Its input V_{REF} is low enough to ensure that the trigger is still in sub-threshold mode when it switches.

The output buffers sharpen the response of the detector, and feed the output back to the Standby input of the subthreshold voltage reference. On triggering of the detector, the low-to-high transition of the output activates the Standby input of the subthreshold voltage reference.

This internal reset has three effects:

1. First, it cuts off the static quiescent current draw of the reference block.
2. Second, the reference output is pulled to ground, which virtually eliminates the static current in the trigger, as its input is no longer at an intermediate voltage.
3. Third, with a grounded input and a falling input, the trigger switches its output back to low at a lower V_{IN} threshold, which provides the detector with hysteresis.

In this way, the switchable voltage reference block allows the detector, once triggered, to remain in a low power mode with a low threshold voltage, without collapsing the sensor output voltage V_{IN}, until V_{IN} returns to the new lower threshold.

This reset of a reference, enabled by feedback in a voltage detector, is not found in the literature. This architecture avoids the use of input voltage dividers and comparators, which would consume significant power.

D. *Transistor-Level Design and Operation of the UB20M's Internal Detector*

The internal detector circuit is shown in Fig. 5. It contains three sub-circuits; the subthreshold voltage reference, the trigger, and the buffers, with $V_{OUT(L)}$ being fed back to the voltage reference.

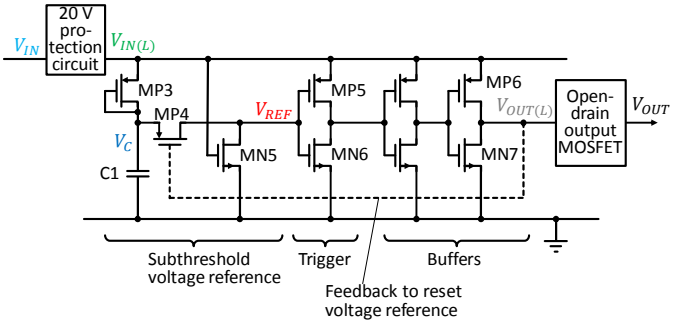

Fig. 5: Internal detector schematic.

The first section of the internal detector of Fig. 5 is the voltage reference, which is made up of MP3, MP4, MN5, and C1. MP4 is controlled by the sub-detector's output $V_{OUT(L)}$, and MN5 by the input $V_{IN(L)}$. The operation of this circuit is explained using the simulation of Fig. 6.

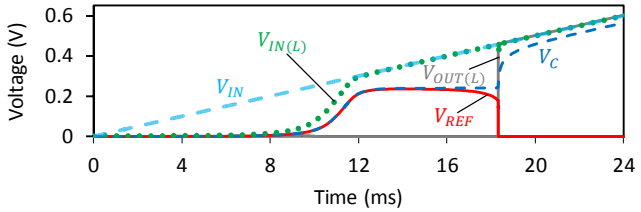

Fig. 6: Simulation of the internal detector of Fig. 5, during a rising input voltage V_{IN}, showing the generation of the temporary reference V_{REF}.

On a rising input voltage V_{IN} of the complete detector system, the sub-detector input $V_{IN(L)}$ is initially held low, as transistors in the 20 V protection circuit are not sufficiently on to conduct the current required to charge C1 and supply the leakage of the sub-detector. At an input V_{IN} of around 0.2 V, the input $V_{IN(L)}$ rises to meet V_{IN}, and the capacitor voltage V_C follows these signals, minus the diode forward voltage drop across MP3. With the output still low and connected to the gate of MP4, MP4 is on and stronger than MN5, therefore V_{REF} follows V_C closely.

As V_{IN} rises further, being connected to the gate of MN5, it turns MN5 on. MN5 starts to draw increased current, resulting in V_{REF} reaching a plateau and ceasing to rise. This plateau is the reference voltage level that determines the input voltage threshold V_{TH} at which the trigger circuit switches.

As the reset input goes high, MP4 is turned off, causing V_{REF} to be shorted to ground via MN5. This also eliminates the static current path in the voltage reference, effectively putting it into a low-power standby mode that consumes around 2 pA.

E. Rectifier Optimised for Efficiency

The RF rectifier uses a single discrete series Schottky diode (SMS7630) to convert the 2.45GHz RF signal into dc as depicted in Fig. 7. The topology uses an input matching circuit that matches the complex impedance of the diode to the impedance of the antenna, i.e., 50 Ω. A low pass output filter is used to eliminate high frequency harmonics and smooth the output dc signal.

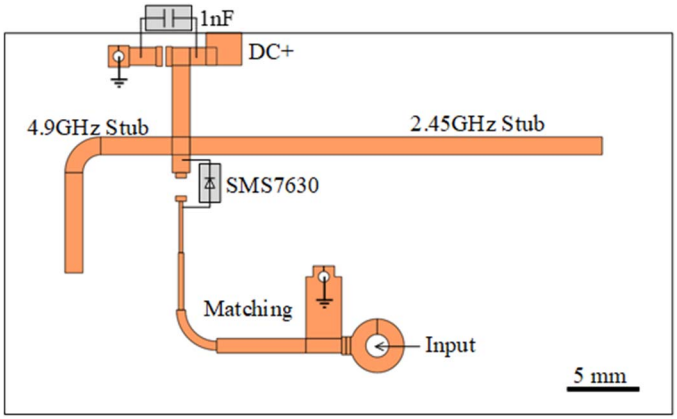

Fig. 7: Layout of the rectifier on Duroid-5880 (35 x 22 mm, layout to scale).

This rectenna achieves a measured RF to dc power conversion efficiency of 32% at -20 dBm with a 5 kΩ resistive load.

Fig. 8 shows the measured open-circuit output voltage of the rectifier against input RF power. The rectifier generates about 10 mV at -33 dBm and 85 mV at -23 dBm.

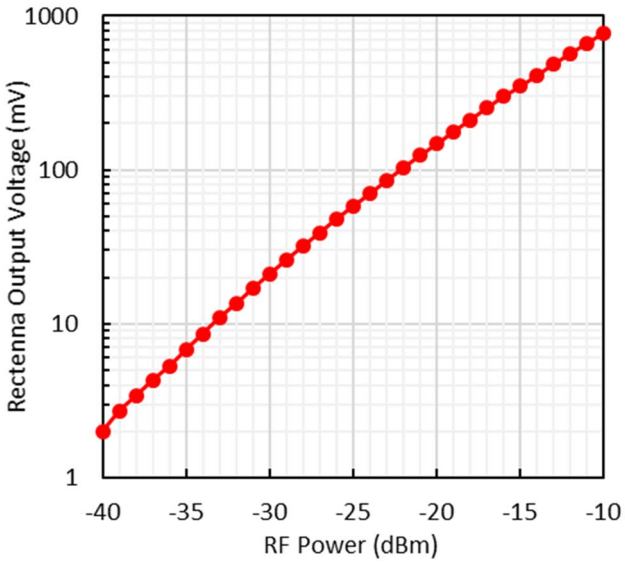

Fig. 8: Open-circuit output voltage of the rectifier versus the RF power level.

F. Boost Converter Design

The boost converter uses the circuit reported in [5], which uses a ring oscillator made from a cascade of two UB20L and one UB20M voltage detectors as the gate driver. The converter operates in discontinuous conduction mode, and therefore its duty ratio can be set so that the converter optimally loads the rectenna (with 5 kΩ), which ensures the rectenna operates at its optimal efficiency.

The control circuit of the boost converter draws 40 nA at 1.2 V from a low power linear regulator. The boost converter including regulator can be entirely self-powered from RF input power levels above -23 dBm.

III. Experimental Results

A. Energy Harvesting

The energy harvesting sub-system of Fig. 1 is evaluated for a wide range of RF power levels. The boost converter receives power from the rectenna and its output is directly connected to a 3 V battery. Fig. 9 shows the measured input voltage of the boost converter and the charging current into the 3V battery. The battery current becomes positive (net charging) from -23 dBm of RF power. Before this point, only the energy harvesting detector consumes power from the battery (1.3 nA at 3 V).

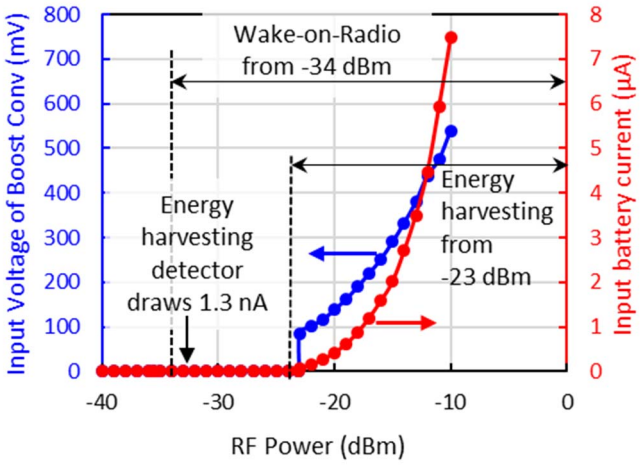

Fig. 9: Measurement of the energy harvesting circuit. The input voltage of the boost converter and the input charging current into the battery are measured against the input RF power.

Fig. 10 shows the total end-to-end power conversion efficiency of the energy harvesting chain. This accounts for all losses including the quiescent consumption of the boost converter and that of a linear regulator, a total of 150 nA at 3V. Efficiency is computed as the ratio of battery charging power to received RF power. The results show that the boost converter is powered off when insufficient RF power is available for harvesting, and that net positive power is harvested from about -23 dBm. The end-to-end efficiency increases from 0 to about 22% at -10 dBm.

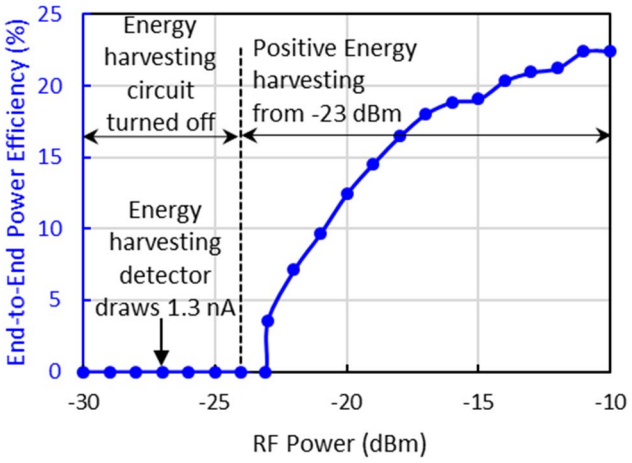

Fig. 10: Measured total end-to-end efficiency of the energy harvesting chain. The detector activates the boost converter at -23 dBm of RF power.

B. Detector Sensitivity, Power Consumption, and Stability over a Typical Battery Voltage Range

The purpose of the following experiments is to measure the triggering sensitivity and power consumption of the detectors in the circuit of Fig. 1.

Fig. 11 shows the time domain waveforms of the input and output voltages of the wake-on-radio detector circuit, for an RF input power pulse of -34 dBm (10 mV dc voltage) lasting 5 ms.

The output of the detector reacts after a delay of 180 µs. After a further delay of around 1 ms, the load resets the input of the voltage detector, which switches off the voltage detector and returns the output to high. A dip in the input voltage appears at 5.5 ms, coinciding with this reset event.

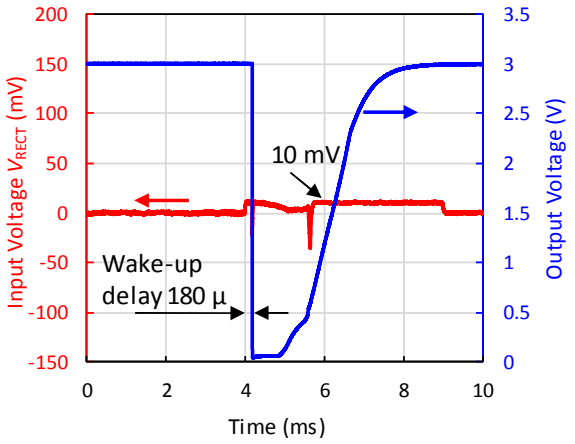

Fig. 11: Measured input and output voltages of the 10 mV wake-on-radio detector, for a -34 dBm RF input pulse lasting 5 ms.

Fig. 12 shows the same experiment carried out on the 85 mV detector, this time using an RF input pulse of -23 dBm. Here, the activation delay is seen to be negligible.

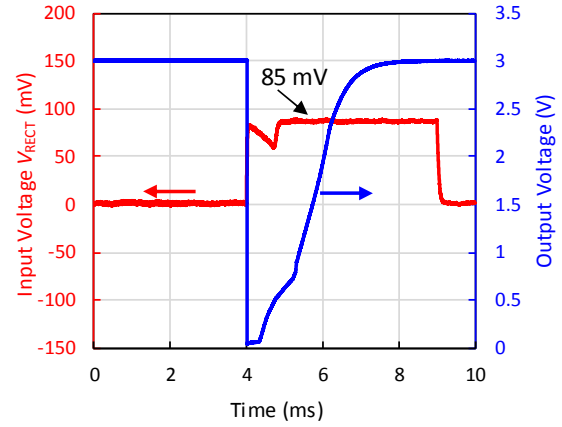

Fig. 12: Measured input and output voltages of the 85 mV wake-on-radio detector, for a -23 dBm RF input pulse lasting 5 ms.

Fig. 13 shows the measured sensitivity and current consumption of the wake-on-radio detector. Both parameters are relatively stable for voltage levels from 2.8 to 3.6 V. The circuit consumes around 10 nW (3.3 nA at 3V).

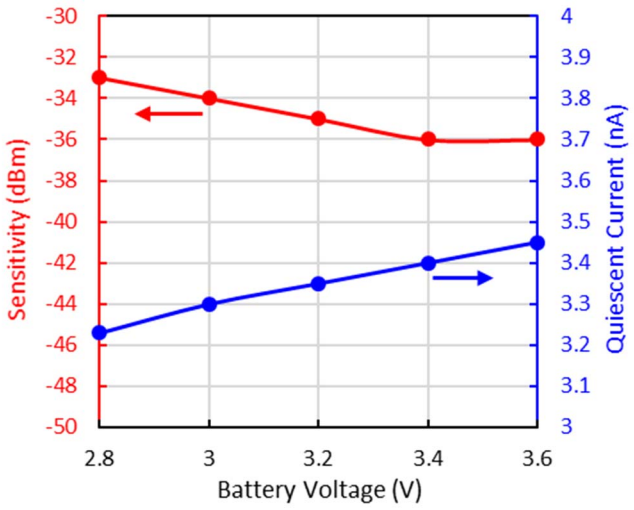

Fig. 13: Measured sensitivity and quiescent current consumption of the 10 mV wake-on-radio detector against battery voltage.

IV. Comparison with State of the Art and Conclusions

The presented detector permits always-on receiving, sensing, and the control of energy harvesting, on a power budget of 10 nW or below. This opens up the possibility of battery life of IoT sensor nodes exceeding 10 years. It allows micro-scale energy harvesters in the nanowatt range to always have a net-positive or neutral power output, in intermittent power environments.

A versatile and low-power detector circuit is presented here, whose detection threshold can be adjusted between 5 mV and 20 V. Between 20 V and 580 mV the detector does not require battery assistance. However, to adjust the detection threshold from 580 mV down to 5 mV, the detector requires increasing bias current. The power consumption against RF sensitivity in dBm is plotted in Fig. 14 (dots).

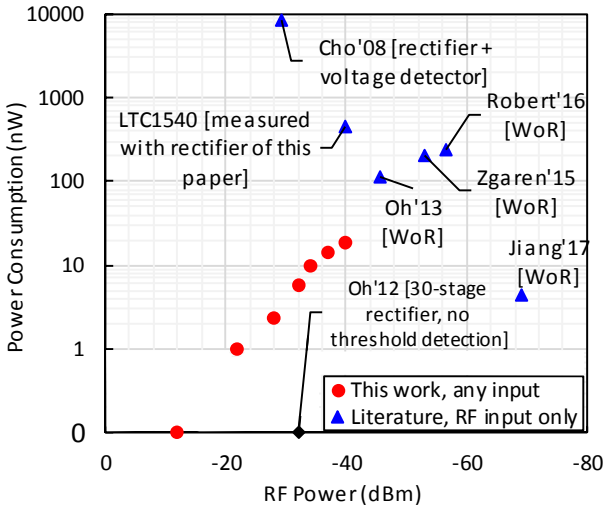

Fig. 14: Comparison of this work against previously reported RF wake-up circuits (Jiang'17 [6], Robert'16 [7], Zgaren'15 [8], Oh'13 [9], Oh'12 [3], Cho'08 [10]) and a commercial low-power comparator (LTC1540).

In addition, this figure also shows the best reported fully-integrated RF wake-on-radio circuits (triangles): Jiang'17 [6], Robert'16 [7], Zgaren'15 [8], Oh'13 [9], and Cho'08 [10]. The highest wake-up sensitivity is achieved in [6], with a combination of an integrated transformer and a powered voltage amplifier, with a quiescent power of 4.5 nW. The rectifiers of all these RF methods listed are optimised for open-circuit voltage, with many, relatively power inefficient, voltage-multiplying stages. By contrast, the rectifier here is optimised for energy harvesting power conversion efficiency, using just one diode. A further advantage of the detection method presented here is that it works with any transient signals, as it does not rely on AC voltage multiplication. Another way of obtaining low-power wake-up from non-AC signals is to use low-power comparators such as the LTC1540, LPV811 and TLV3691. For the same sensitivity, at typical rail voltages, these use over 40× more power than the partially discreet implementation presented here. Also, they do not permit the further reduction in power to nW or even below, at the expense of sensitivity. It is expected that the full integration of the entire circuit presented here will further improve sensitivity, stability, and reduce power consumption.

References

[1] C. H. P. Lorenz *et al.*, "Breaking the Efficiency Barrier for Ambient Microwave Power Harvesting With Heterojunction Backward Tunnel Diodes," *IEEE Trans. Microw. Theory Tech.*, vol. 63, no. 12, pp. 4544–4555, Dec. 2015.

[2] S. Bandyopadhyay, P. P. Mercier, A. C. Lysaght, K. M. Stankovic, and A. P. Chandrakasan, "A 1.1 nW Energy-Harvesting System with 544 pW Quiescent Power for Next-Generation Implants," *IEEE J. Solid-State Circuits*, vol. 49, no. 12, pp. 2812–2824, Dec. 2014.

[3] S. Oh and D. D. Wentzloff, "A −32dBm sensitivity RF power harvester in 130nm CMOS," in *2012 IEEE Radio Frequency Integrated Circuits Symposium*, 2012, pp. 483–486.

[4] "UB20M datasheet," *Sensor Driven Ltd*. [Online]. Available: www.sensor-driven.com.

[5] S.-E. Adami, "A Flexible 2.45 GHz Power Harvesting Wristband with Net System Output from -24.3 dBm of RF Power," *IEEE Trans. Microw. Theory Tech.*, vol. xx, no. xx, pp. xxxx–xxxx, xxx 2017.

[6] H. Jiang *et al.*, "A 4.5nW Wake-Up Radio with -69dBm Sensitivity," in *2017 IEEE International Solid-State Circuits Conference (ISSCC)*, 2017, pp. 416–417.

[7] N. E. Roberts *et al.*, "A 236nW −56.5dBm-sensitivity bluetooth low-energy wakeup receiver with energy harvesting in 65nm CMOS," in *2016 IEEE International Solid-State Circuits Conference (ISSCC)*, 2016, pp. 450–451.

[8] M. Zgaren and M. Sawan, "A Low-Power Dual-Injection-Locked RF Receiver With FSK-to-OOK Conversion for Biomedical Implants," *IEEE Trans. Circuits Syst. Regul. Pap.*, vol. 62, no. 11, pp. 2748–2758, Nov. 2015.

[9] S. Oh, N. E. Roberts, and D. D. Wentzloff, "A 116nW multi-band wake-up receiver with 31-bit correlator and interference rejection," in *2013 IEEE Custom Integrated Circuits Conference (CICC)*, 2013, pp. 1–4.

[10] H. Cho *et al.*, "Highly sensitive CMOS passive wake-up circuit," in *Microwave Conference, 2008. APMC 2008. Asia-Pacific*, 2008, pp. 1–4.

[11] J. Masuch, M. Delgado-Restituto, D. Milosevic, and P. Baltus, "Co-Integration of an RF Energy Harvester Into a 2.4 GHz Transceiver," *IEEE J. Solid-State Circuits*, vol. 48, no. 7, pp. 1565–1574, Jul. 2013.